Fuel 143 (2015) 361–372

Contents lists available at ScienceDirect

Fuel

journal homepage: www.elsevier.com/locate/fuel

Techno-economic performance analysis of biofuel production and miniature electric power generation from biomass fast pyrolysis and bio-oil upgrading

Mobolaji B. Shemfe, Sai Gu *, Panneerselvam Ranganathan

Centre for Bioenergy & Resource Management, Cranfield University, Bedford, Bedfordshire MK43 0AL, UK

HIGHLIGHTS

- Predictive process model of a biomass fast pyrolysis and bio-oil upgrading plant.
- Evaluation of energy efficiency and the impact of integrating power generation equipment.
- Evaluation of the impact of biomass composition on fast pyrolysis products and bio-fuel yield.
- Evaluation of the impact of initial biomass moisture content on power generation.
- Economic evaluation and economic sensitivity to key process parameters.

ARTICLE INFO

Article history:
Received 8 September 2014
Received in revised form 11 November 2014
Accepted 24 November 2014
Available online 5 December 2014

Keywords:
Fast pyrolysis
Techno-economic analysis
Process modelling
Biomass
Bio-oil upgrading

ABSTRACT

The techno-economic performance analysis of biofuel production and electric power generation from biomass fast pyrolysis and bio-oil hydroprocessing is explored through process simulation. In this work, a process model of 72 MT/day pine wood fast pyrolysis and bio-oil hydroprocessing plant was developed with rate based chemical reactions using Aspen Plus® process simulator. It was observed from simulation results that 1 kg s^{-1} pine $wood_{db}$ generate 0.64 kg s^{-1} bio-oil, 0.22 kg s^{-1} gas and 0.14 kg s^{-1} char. Simulation results also show that the energy required for drying and fast pyrolysis operations can be provided from the combustion of pyrolysis by-products, mainly, char and non-condensable gas with sufficient residual energy for miniature electric power generation. The intermediate bio-oil product from the fast pyrolysis process is upgraded into gasoline and diesel via a two-stage hydrotreating process, which was implemented by a pseudo-first order reaction of lumped bio-oil species followed by the hydrocracking process in this work. Simulation results indicate that about 0.24 kg s^{-1} of gasoline and diesel range products and 96 W of electric power can be produced from 1 kg s^{-1} pine $wood_{db}$. The effect of initial biomass moisture content on the amount of electric power generated and the effect of biomass feed composition on product yields were also reported in this study. Aspen Process Economic Analyser® was used for equipment sizing and cost estimation for an *n*th plant and the product value was estimated from discounted cash flow analysis assuming the plant operates for 20 years at a 10% annual discount rate. Economic analysis indicates that the plant will require £16.6 million of capital investment and product value is estimated at £6.25/GGE. Furthermore, the effect of key process and economic parameters on product value and the impact of electric power generation equipment on capital cost and energy efficiency were also discussed in this study.

1. Introduction

Crude oil remains the main source of transport fuel and is projected to continue to dominate the fuel market over the next two decades [1]. However, biofuels are being rapidly deployed globally as a sustainable substitute in an effort to reduce the world's dependence on crude oil due to the environmental implications of burning fossil fuels as well as stringent regulation on carbon emissions [2–4].

Biomass is mainly converted into biofuels via biochemical and thermochemical routes. While biochemical conversion processes have been demonstrated on a commercial scale, they are economically unsustainable and exert market pressure on food crops and

* Corresponding author.
E-mail address: s.gu@cranfield.ac.uk (S. Gu).

http://dx.doi.org/10.1016/j.fuel.2014.11.078
0016-2361/

biodiversity [4,5]. On the other hand, thermochemical conversion processes which include pyrolysis, gasification and hydrothermal liquefaction have great potential for producing advanced biofuels from non-food sources that do not compete with food sources [3,4]. However, the products obtained from these processes vary in physical properties and chemical composition, and consequently present unique technical and economic challenges [6].

Among the various thermochemical processes biomass fast pyrolysis presents the best case for maximising bio-oil yields which can be subsequently upgraded into transport fuels [7,8]. Fast pyrolysis involves the anaerobic thermochemical decomposition of lignocellulosic biomass from 450 °C to about 650 °C and at a short vapour residence time of 2 s to produce liquids (bio-oil), solids (char and ash) and non-condensable gas (NCG). The fast pyrolysis by-products (char and NCG) can be combusted to provide all the energy required to drive biomass pyrolysis and drying operations, while the combustion waste heat can be exported or utilised for supplementary electric power generation [9]. The bio-oil product has a high composition of water and oxygenated organic compounds. As a result, it exhibits acidic and corrosive properties and has a relatively low HHV compared with conventional petroleum-derived fuels, making it unusable in internal combustion engines [9].

Bio-oil can be upgraded into naphtha-range transport fuels via two major conventional refinery operations that have been broadly identified and reviewed in literature, namely, hydroprocessing and catalytic cracking processes [6,10,11].

Hydroprocessing encompasses two main hydrogen intensive processes namely, hydrotreating/hydrodeoxygenation and hydrocracking. Hydrotreating/hydrodeoxygenation involves the stabilisation and selective removal of oxygen from untreated bio-oil through its catalytic reaction with hydrogen over alumina-supported, sulfided CoMo or NiMo catalysts or noble metal catalysts, while hydrocracking involves the simultaneous scission and hydrogenation of heavy aromatic and naphthenic molecules into lighter aliphatic and aromatic molecules [6,9,10].

Although various fast pyrolysis reactor configurations have been demonstrated on pilot scales in worldwide, the bubbling fluid bed reactor has been identified as the best in terms of ease of scalability, biomass heat transfer efficiency and temperature control efficiency [9]. The production of transport biofuels from the fast pyrolysis of biomass is yet to be commercialised due to the high level of investment required for production and a lack of competitiveness with fossil fuels. This makes process modelling and simulation an indispensable tool for investigating process performance and the impact of process and economic parameters on its economic viability.

The supporting solid operations required for the fast pyrolysis process consisting of grinding and drying operations are currently inadequately described in available software. Moreover, existing process models specify the product yield compositions for the pyrolysis reactor without accounting for the effect of temperature and chemical kinetics due to the complexity of the thermochemical reaction kinetics involved. In addition, most available reaction models in literature are descriptive of the intra-particle relationship rather than predictive of the product distribution [12]. As a result, a high fidelity process model is required for the analysis of the whole process with minimal assumptions.

There are several studies on the techno-economic analysis of biomass fast pyrolysis for bio-oil production available in literature; however, very few studies consider the upgrading of bio-oil into transport fuels or quantify the amount of electric power capable of being generated from fast pyrolysis by-products [13–16]. These studies report bio-oil costs ranging from US$0.62/gal to US$1.40/gal and capital costs ranging from US$7.8 to US$143 million over a 240 MT/day to 1000 MT/day plant capacity range. The significant disparity in the bio-oil costs from these studies can be attributed to the fact that different assumptions were adopted in each study.

Few researchers have conducted techno-economic analysis of the fast pyrolysis process and bio-oil hydroprocessing for transport fuel production [17,18] via a process simulation platform. In 2009, Jones et al. [17] conducted a design case study to evaluate the production of hydrocarbon biofuel from a 2000 MT/day plant of hybrid poplar wood chips. In their study, capital expenditure of US$303 million was estimated with a minimum fuel selling price of US$2.04. In 2010, another techno-economic analysis was also conducted by Wright et al. [18] on a 2000 MT/day of corn stover fast pyrolysis plant and subsequent bio-oil upgrading via hydrotreating and hydrocracking processes to obtain fuel product value and capital costs at US$2.11/gal/US$287 million and US$3.09/gal/US$200 million for hydrogen purchase and *in-situ* hydrogen production scenarios respectively.

In this study, a 72 MT/day fast pyrolysis plant of pine wood and subsequent bio-oil hydroprocessing is modelled based on rate based chemical reactions to evaluate the techno-economic performance of the process. Particularly, more emphasis is made on the detailed modelling of process equipment to ensure realistic model results. The fast pyrolysis reactor model is developed using rate based multi-step chemical reactions [19] in Aspen Plus® process simulator and validated with experimental results reported by Wang et al. [20]. Auxiliary processes consisting of grinding, screening, drying, combustion, bio-oil collection system and power generation are modelled using design specifications with the appropriate thermodynamic property methods. The hydrotreating process is modelled adopting a pseudo-first order reaction kinetic model over Pt/Al_2O_3 catalysts [21]. Based on validated process models, the effect of process and economic input parameters on the process and economic performance are further explored.

2. Material and methods

2.1. Process description

The overall process of transport fuel production from biomass is divided into eight main processing areas described by the generalised process flow diagram in Fig. 1. In the feed pre-treatment processing area (A100), the feed undergoes grinding and drying operations to meet the minimum feed requirement of 2 mm diameter and 10% moisture content in the pyrolysis reactor. Next, it is passed on to the fast pyrolysis area (A200), where the biomass feed is thermochemically converted in the absence of oxygen into NCG, hot pyrolysis vapours and char. The product from the fast pyrolysis reactor is then fed into the solid removal section area (A300), where char is separated from pyrolysis vapour and NCG before the pyrolysis vapour is subsequently condensed. The condensation of the pyrolysis vapours is achieved by quenching it into liquid in the bio-oil recovery section (A400), which contains vapour quenching process units. NCG and char separated from bio-oil are then combusted in the combustion area (A500) to generate the energy (hot flue gas) required for biomass drying and fast pyrolysis processes. The residual heat from combustion, if any, is used to generate the high pressure steam for power generation (A600). The bio-oil is upgraded into gasoline and diesel fraction products in the bio-oil hydroprocessing area (A700) containing hydrotreating and hydrocracking processes. Hydrogen required for hydroprocessing is generated in the hydrogen generation section (A800).

2.2. Model development

The biomass fast pyrolysis model is implemented in Aspen Plus® V8.2 using its improved solid modelling capabilities. The main model assumptions adopted in this study are presented in Table 1. The comprehensive process flow diagrams for bio-oil

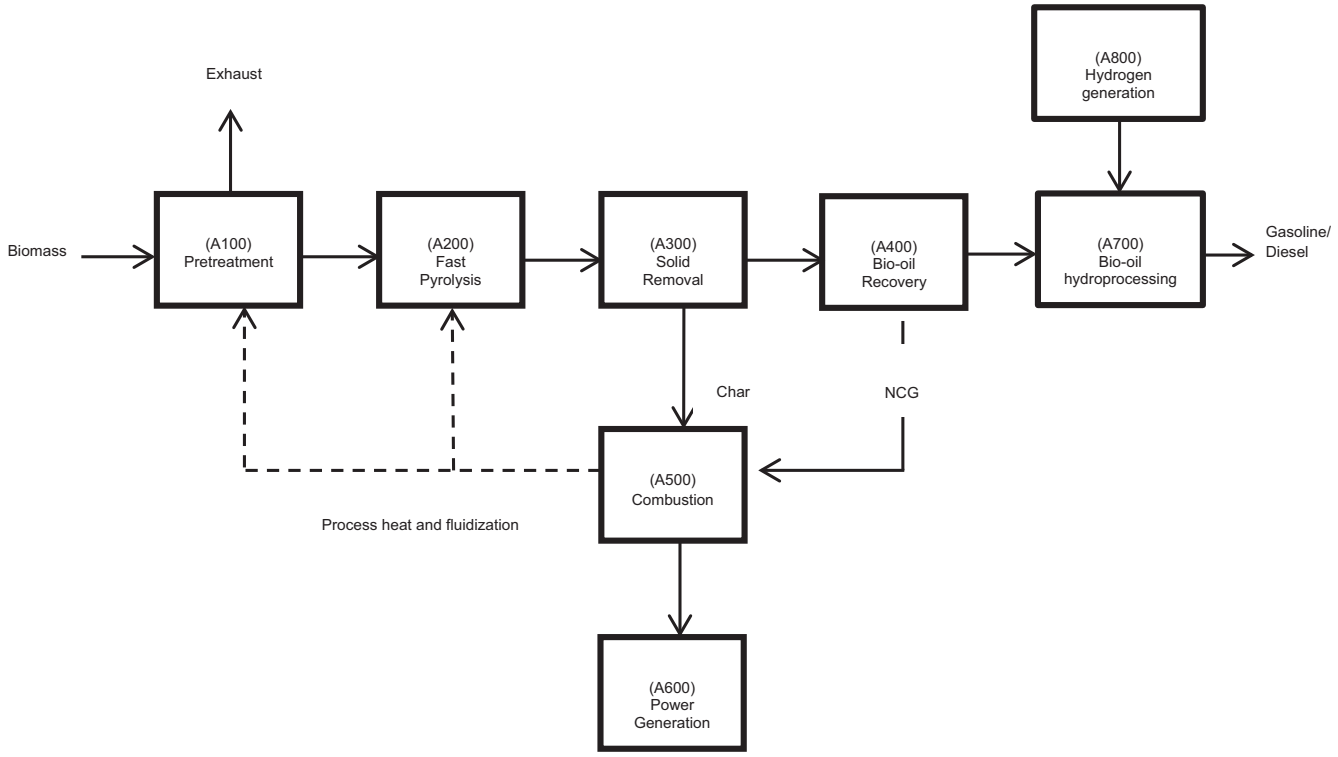

Fig. 1. Generalised process flow diagram.

production and electric power generation (A100–A600) and bio-oil hydroprocessing and hydrogen generation (A700–A800) are shown in Figs. 2 and 3 respectively.

2.2.1. Pretreatment section (A100)

Wet pine wood stream (CHR-1) supplied at 20 mm diameter is fed into a multiple roll crusher (CHR) in which the particle size is reduced to 2 mm and followed by a screen (SCRN) for particle separation. The exiting wet biomass stream (CHR-2) with initial moisture content of 25% is then fed into a rotary dryer (DRYER) at an operating temperature of 300 °C to reduce its moisture content. A rotary dryer was adopted in the model due to its flexibility in operation, low maintenance costs and high operating temperature range [22]. The energy required for drying is supplied by a fraction of flue gas (DYR-FLS) from the combustor (CB-BUR) which exits the dryer as a mixture of hot air and water vapour (DR-4), while the dried pine wood exits the dryer with a 10% moisture content (DR-3). The dried biomass feed then goes into the fluidised bed reactor.

2.2.2. Pyrolysis section (A200)

Three model blocks (PYR-DEC, PYR-FLD and PYR-RXN) were used to model a bubbling fluidised bed pyrolysis reactor. In the yield reactor (PYR-DEC), biomass is fragmented into its subcomponents (cellulose, hemicellulose and lignin). The fluidised bed (PYR-FLD) is used to model the reactor's fluid dynamics with a specified bed pressure drop of 150 mbar, an inert sand bed to biomass particle mass ratio of 1:1.25 and a reactor temperature of 500 °C. The reactor temperature is controlled by varying the fluidizing gas flow rate comprising inert nitrogen gas (FLGAS-1). The transport disengagement height in the fluidized bed is calculated using Fournol et al. [23] empirical correlation for FCC powders with particles classified as Geldart B particles. The process heat and fluidizing gas for the fluid bed is supplied at 863 °C with a 1:1 mass ratio to biomass feed. The rate based chemical reactions of each biomass subcomponent was modelled by the CSTR (PYR-RXN) using multi-step reactions kinetics of biomass pyrolysis developed by Ranzi et al. [19]. The reactor products comprising a mixture of hot

Table 1
Process assumptions.

Process section		Process assumption
Bio-oil production and power generation	Pretreatment (A100)	Biomass size as received is 20 mm with 25% initial moisture content
	Fast pyrolysis (A200)	Process heat supplied by NCG and char combustion with nitrogen as the fluidizing gas
	Solid removal (A300)	Solid products are separated from the hot vapours stream by high efficiency cyclones at 95% separation efficiency
	Bio-oil recovery (A400)	A direct contact spray tower used for rapid quenching of bio-vapours to 49 °C using previously stored bio-oil as quench liquid
	Combustion (A500)	Char is combusted in 60% theoretical air to obtain 1269 °C to prevent ash melting at adiabatic flame temperature up to 1700 °C
	Power generation (A600)	Steam Rankine cycle with an isentropic efficiency of 80% and mechanical efficiency of 95%
Bio-oil hydroprocessing	Bio-oil hydroprocessing (A700)	2 Stage hydrotreating reactions over Pt/Al_2O_3 catalysts
	Hydrogen generation (A800)	Hydrogen generated from the reforming of 40 wt.% of the bio-oil aqueous phase and supplementary natural gas

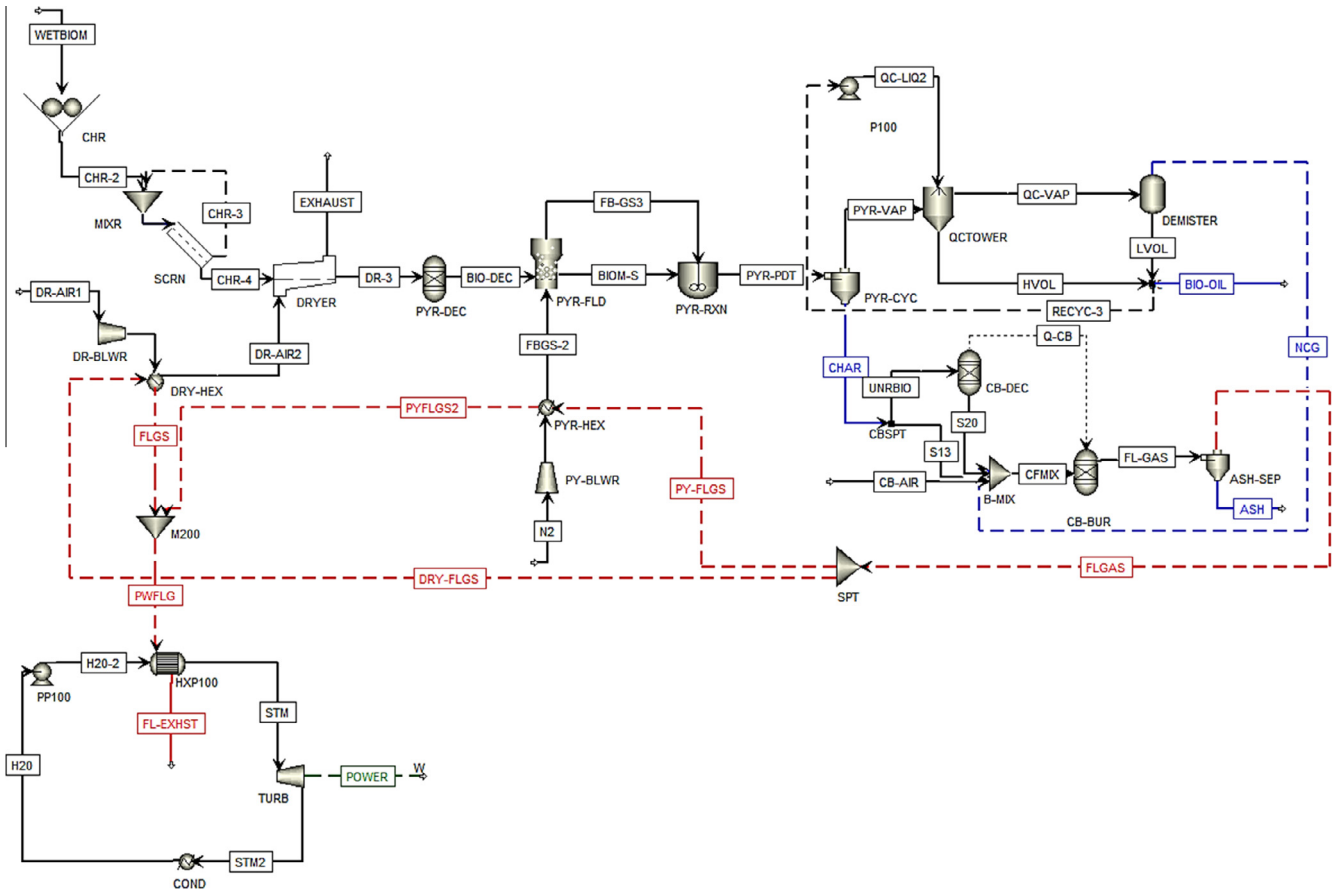

Fig. 2. Fast pyrolysis process flowsheet (A100–A600).

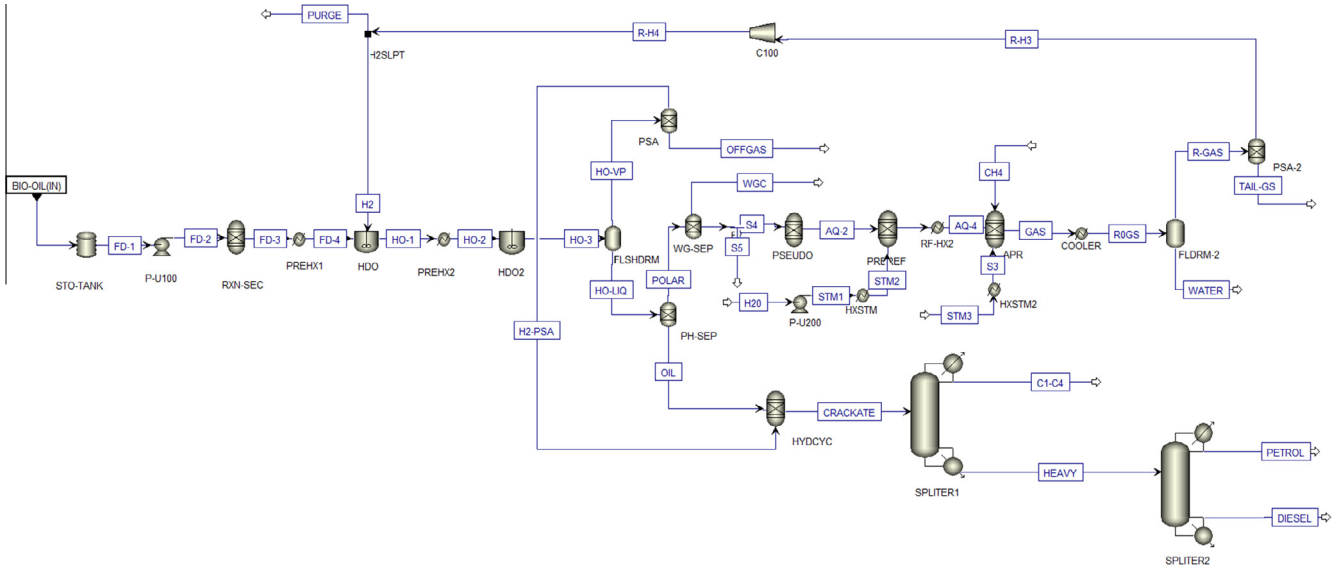

Fig. 3. Bio-oil hydroprocessing and hydrogen production flowsheet (A700–A800).

vapours, gas and solids are sent into a cyclone (SP-CYC) to separate the solids particles (PYR-SD) from the mixture.

2.2.3. Products separation and recovery (A300-A400)

Char and unreacted biomass (PYR-SD) are separated from the hot vapour and gas stream (PYR-VAP) in a cyclone (PYR-CYC) at 95% separation efficiency and the separated solids are subsequently fed into a combustor. The remaining stream of hot vapour and gas (PYR-VAP) at 500 °C goes into a spray tower (QUENCH), where the hot vapours are quenched to 49 °C using previously stored bio-oil liquid (QC-LIQ) at 25 °C as the quench liquid with a mass ratio of 10:1 to the hot vapour stream. The spray tower is modelled using the Non-random two-liquid activity coefficient model with Nothnagel equation of state for the vapour phase

model (NRTL-NTH). NCG and the remaining condensable vapours (QC-GAS) then go into a high pressure vapour–liquid separator (DEMISTER) operated at 10 bar to collect the bio-oil vapours entrained as aerosol particles. An electrostatic precipitator (ESP) could be used instead, but this was precluded due to its very high equipment cost [9]. The resultant dry NCG goes to a combustor along with char while the quenched bio-oil is sent for further upgrading in the bio-oil hydroprocessing section (A700-A800).

2.2.4. Combustion section (A500)

The combustion section is modelled by a yield reactor (CB-DEC) and a Gibbs reactor (CB-BUR). Unreacted biomass separated from the cyclone goes into the yield reactor (CB-DEC) where it is decomposed into its constituent elements before it is fed into the Gibbs reactor (CB-BUR) along with char (assumed to be 100% carbon in elemental constitution) and NCG. The Gibbs reactor calculates the multi-phase chemical equilibrium by minimising Gibbs free energy and it was modelled using the Peng–Robinson–Boston–Mathias (PR–BM) equation of state. Although a maximum temperature of 1700 °C can be achieved at complete combustion, the fuel mixture of solids and NCG are combusted in 60% theoretical air at a combustion temperature of 1269 °C in order to mitigate ash melting and prevent material failure at severe temperatures. Ash is separated from the resultant combustion gases by a hot cyclone (ASH-SEP). The resultant flue gas (FL-GAS) is sent into a splitter (GAS-SPLIT), where it is divided into two streams (PYR-FLGS) and (DRY-FLGS). These are supplying heat for the feed nitrogen gas, which goes to the fluidized bed pyrolysis reactor and for the feed air, which goes to the dryer via two-stream heat exchangers. The residual flue gas heat at 800 °C is used for superheated steam generation for subsequent electric power generation.

2.2.5. Power generation (A600)

The residual heat from combustion is exchanged with water in a two-stream heat exchanger to generate superheated steam at 450 °C and 50 bar with an outlet flue gas temperature of 90 °C. The superheated steam is supplied to a steam turbine (TURB), modelled at 80% isentropic efficiency and mechanical efficiency of 95% to generate electric power (POWER).

2.2.6. Bio-oil hydroprocessing (A700)

Bio-oil product (BIO-OIL) is hydrotreated in a two-stage hydrotreating process over Pt/Al_2O_3 catalyst due to increased aromatic yield compared with conventional catalysts such as sulfided $CoMo/Al_2O_3$ and sulfided $Ni–Mo/Al_2O_3$ [21]. The two-stage hydrotreating process is modelled by two CSTRs (HDO1 and HDO2) using a pseudo-first order reaction model of lumped bio-oil species based on previously reported study [21]. A yield reactor is introduced afore the hydrotreaters to lump bio-oil into five pseudo-components, namely, light non-volatile; heavy non-volatile; phenolics; aromatics + alkanes; Coke + H_2O + outlet gases. Since all chemical compounds in the bio-oil are primarily composed of carbon, hydrogen and oxygen, the pseudo components are grouped solely based on their molecular weights and functional groups. The lumped bio-oil species go into the first hydrotreater (HDO-1) operating at mild conditions 270 °C and 87 bar and is then fed into the second hydrotreating unit (HDO-2) under more severe operating temperature 383 °C and 87 bar in a hydrogen-rich environment of 5 wt.% [24]. The weight hourly space velocity (WHSV) for the reactors is specified as 2 h^{-1}. The hydrotreating product (HO-P) is sent into a flash drum (F-DRUM) operated at 40 °C and 20 bar to separate hydrotreater gas (HO-VP) from hydrotreated oil (HO-LQ).

Hydrotreated oil goes into a phase separator (PH-SEP) to separate the polar phase from the non-polar phase with the former going into a reformer to generate hydrogen and the latter fed to a hydrocracker (HYD-CYC) to obtain gasoline and diesel range fuels. The polar phase accounts for 69 wt.% of the bio-oil while the oil phase accounts for the remaining 31 wt.%. Due to lack of adequate knowledge of bio-oil hydrocracking reaction kinetics, a yield reactor was adopted at 104.3 bar and 400 °C while the reactor yields are specified based on hydrocracking product composition from the work conducted by Elliot et al. [25]. The hydrocrackates are finally separated into gasoline and diesel products in a product fractionator (SPLITER1 and SPLITER2).

2.2.7. Hydrogen production (A800)

The aqueous phase reforming unit entails two reactors: a pre-reformer (PRFM) and an aqueous phase reformer (APR) represented by two Gibbs reactors based on UOP bio-oil aqueous reforming process scheme [24]. This study assumes 40% of the polar phase goes to the pre-reformer. The pre-reformer is operated at 426 °C to generate synthesis gas which is subsequently fed to the aqueous reformer along with supplementary natural gas to undergo equilibrium reforming reactions with superheated steam at 270 °C. The target hydrogen product flow rate is determined by varying the flow rate of superheated steam required in the reformer using a design specification block. The product from the aqueous reformer goes into a flash drum where the gas mixture is separated from the water vapour and then the gas mixture is sent to a pressure swing adsorption (PSA) unit, which separates the hydrogen from the gas mixture, which is then recycled for hydroprocessing.

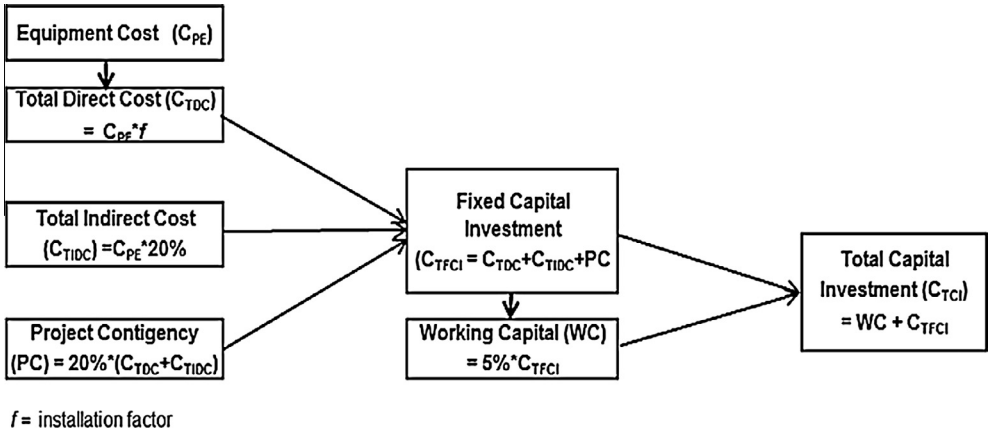

Fig. 4. Capital investment estimation methodology.

Table 2
Economic inputs and assumptions.

Parameter	Value	Parameter	Value
Pine wood cost (£/ton) [26]	90	Annual RRR (%)	10
5 wt.% Pt/Al_2O_3 catalyst cost (£/kg) [27]	4500	Project contingency (%)	20
Ash disposal cost (£/ton) [18]	0.11	Project economic life (year)	20
Supplementary natural gas (£/GJ)	3.59	Working capital (%)	5
Electricity price (£/kW h) [26]	0.15	Depreciation method	Straight Line
PSA operating cost (£/ton)	21	Plant overhead (%)	50
Project capital and product escalation (%)	5.00	Operating cost escalation (%)	3

Table 3
Proximate and chemical composition of pine wood [28].

Proximate analysis	$wt.\%_{ar}$	Subcomponent composition	$wt.\%_{ad}$
Moisture content	25	Cellulose	42
Fixed carbon	20	Hemicellulose	23
Volatile matter	55	Lignin	24
Ash	0.7	Water	10

2.3. Process economics

Equipment cost estimation and sizing is carried out in Aspen Process Economic Analyser® V8.2 (APEA) based on Q1. 2013 cost data. APEA maps unit operations from Aspen Plus® flow sheet to equipment cost models, which in turn size them based on relevant design codes and estimate the Purchased Equipment Costs (C_{PE}) and Total Direct Costs (C_{TDC}) based on vendor quotes. The costs of the equipment that cannot be estimated from APEA are estimated from Eq. (1) using costs reported by Wright et al. [18] as the basis for estimation.

$$C_1 = C_0 * \left(\frac{S_1}{S_0}\right)^n \quad (1)$$

where C_1 is the new estimated cost with S_1 capacity, C_o is the initial equipment cost with S_0 capacity and n is the scaling factor, typically 0.6.

The hypothetical plant is situated in North-Western England, hence material costs and wage rates in the UK are applied and costs are given in Pound Sterling. The capital investment estimation methodology adopted in this study for the nth plant scenario is illustrated in Fig. 4. Total Indirect Cost (C_{TIDC}), which includes design and engineering costs and contractor's fees, is taken as 20% of C_{PE}. project contingency (PC) is taken as 20% of the sum of Total Direct and Indirect Costs. Total Fixed Capital Investment (C_{TFCI}) is estimated from the sum of C_{TDC}, C_{TIDC} and PC, and total capital investment (C_{TCI}) is estimated from the summation of working capital (5% of C_{TFCI}) and C_{TFCI}.

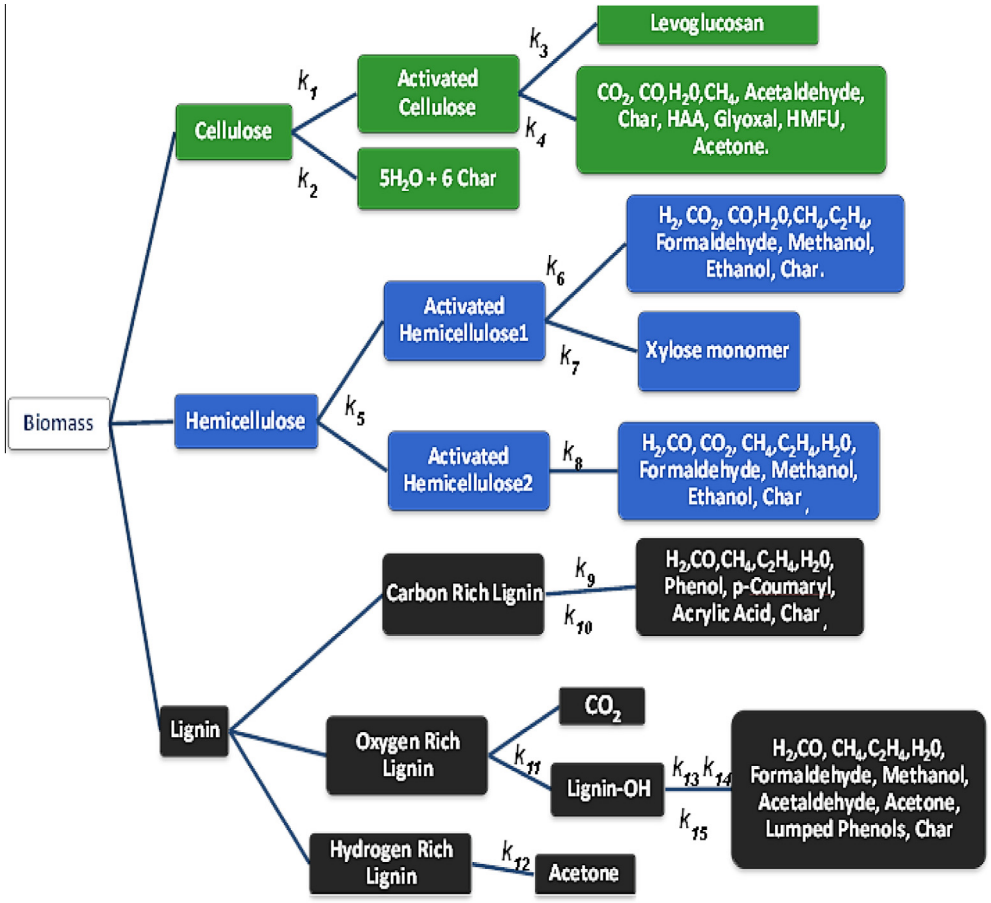

Fig. 5. Multi-step reaction pathways for biomass pyrolysis [19].

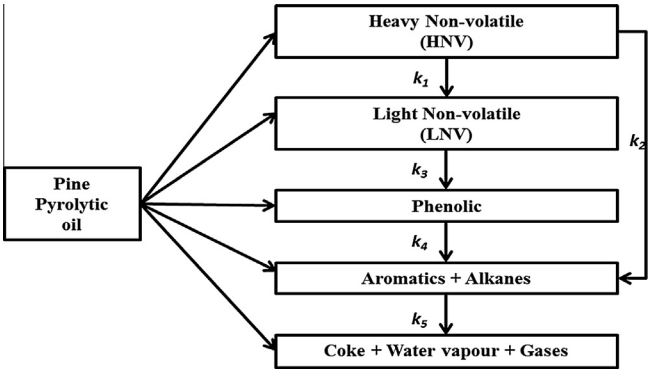

Fig. 6. Reaction pathways for the hydrotreating of lumped bio-oil species.

Total operating cost is also estimated from APEA, including operating labour cost, raw material cost, hydroprocessing catalyst cost, reformer catalyst cost, PSA packing, ash disposal cost, maintenance cost, utilities cost, operating charges, capital charges, plant overhead and general and administrative (G & A) costs. For discounted cash flow (DCF) analysis, the following investment parameters are assumed: tax rate of 40%, required rate of return (RRR) 10% and 20 years project economic life. The main economic inputs and assumptions adopted for economic analysis are presented in Table 2.

2.4. Model inputs

The model inputs including proximate analysis of pine wood and biomass subcomponent composition are shown in Table 3. Multi-step reaction kinetics of biomass pyrolysis as shown in Fig. 5 was implemented in this work. Bio-oil hydrotreating reaction kinetics was implemented by lumping approach of bio-oil components, which is shown in Fig. 6. The kinetic parameters for biomass pyrolysis and bio-oil hydrotreating reactions are given in Tables 4 and 5 respectively.

3. Results and discussion

3.1. Model validation

The fast pyrolysis model developed in this study is validated with experimental work by Wang et al. [20] on a fluidized bed pyrolysis reactor using pine wood feedstock. The comparison between fast pyrolysis reactor model results and experimental measurements of pyrolysis products as a function of reaction temperature is depicted in Fig. 7. It was observed that pyrolysis

Table 5
Bio-oil hydrotreating reactions [21].

	Reaction	A (s^{-1})	E (kj/mol)
1	Heavy non-volatiles → light non-volatile	6.40×10	78
2	Heavy non-volatiles → [alkanes + aromatics]	1.26×10^3	91.8
3	Light non-volatiles → phenolics	1.38×10^2	80.6
4	Phenolics → [alkanes + aromatics]	1.58×10	62.3
5	[Alkanes + aromatics] → [coke + water + gases]	7.75×10	75

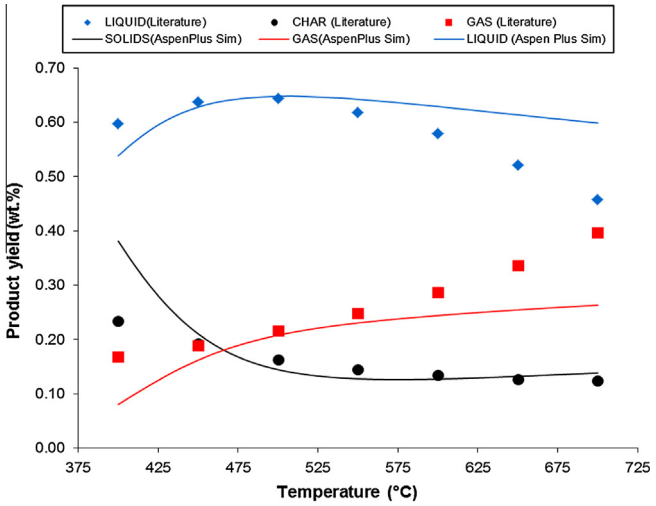

Fig. 7. Aspen Plus simulation results vs. experimental data from [20] as a function of reactor temperature.

reaction model results agree considerably with experimental data, particularly between 475 °C and 550 °C, which is the typical temperature range at which bio-oil yield is highest. The hydrotreating reactor model result was validated with experimental work by Sheu et al. [21] at temperature of 400 °C, pressure of 87.2 bar and WHSV of 2 h^{-1} over Pt/Al_2O_3 catalyst as shown in Table 6. It can be seen from Table 6 that hydrotreating model results are in adequate agreement with experimental data. The summary of simulation results from the validated model is presented in Table 7.

The moisture content of the biomass feed after undergoing drying operation is reduced to 10% while the evaporated moisture from the biomass is purged with dryer exhaust containing 499 kg/h water vapour. The product yield from the pyrolysis process is 22 wt.%, 64 wt.% and 14 wt.% for NCG, bio-oil and char respectively. These values are comparable to previously published studies [7–9]. The amount of water in the bio-oil product is

Table 4
Pyrolysis chemical reactions [19].

	Reaction	A (s^{-1})	E (kj/mol)
1	Cell → CellA	8×10^{13}	192.5
2	Cell → $5H_2O$ + 6Char	8×10^7	125.5
3	CellA → Levoglucosan	4T	41.8
4	CellA → 0.95HAA + 0.25Glyoxal + 0.2Acetaldehyde + 0.25HMFU + 0.2Acetone + $0.16CO_2$ + 0.23CO + $0.9H_2O$ + $0.1CH_4$ + 0.61Char	1×10^9	133.9
5	HCell → 0.4HCell1 + 0.6HCell2	1×10^{10}	12.9.7
6	HCell → $0.75H_2$ + $0.8CO_2$ + 1.4CO + 0.5Formaldehyde	3×10^9	113
7	HCell1 → Xylan	3T	46
8	HCell2 → CO_2 + $0.5CH_4$ + $0.25C_2H_4$ + 0.8CO + $0.8H_2$ + 0.7Formaldehyde + 0.25Methanol + 0.125Ethanol + $0.125H_2O$ + Char	1×10^{10}	138.1
9	Lig_C → $0.35Lig_{CC}$ + 0.1pCourmaryl + 0.08Phenol + $0.14C_2H_4$ + H_2O + $0.495CH_4$ + $0.32CO_2$ + CO + H_2 + 5.735Char	4×10^{15}	202.9
10	Lig_H → LigOH + Acetone	2×10^{13}	156.9
11	Lig_O → LigOH + CO_2	1×10^9	106.7
12	Lig_{CC} → 0.3pCoumaryl + 0.2Phenol + 0.35Acrylic + $0.7H_2O$ + $0.65CH_4$ + $0.6C_2H_4$ + 1.8CO + H_2 + 6.4Char	5×10^6	131.8
13	Lig_{OH} → Lig + H_2O + Methanol + $0.45CH_4$ + $0.2C_2H_4$ + 2CO + $0.7H_2$ + 4.15Char	3×10^8	125.5
14	Lig → Lumped phenol	8T	50.2
15	Lig → H_2O + 2CO + 0.2Formaldehyde + 0.4Methanol + 0.2Acetaldehyde + 0.2Acetone + $0.6CH_4$ + $0.65C_2H_4$ + $0.5H_2$ + 5.5Char	1.2×10^9	125.5

Table 6
Hydrotreated bio-oil results validated with experimental measurements.

Lumped bio-oil components	HT model (wt.%)	Experiment [21] (wt.%)	Percentage error (%)
Heavy nonvolatiles	22.94	24.57	6.63
Light nonvolatiles	29.83	29.41	1.43
Phenolics	10.55	10.63	0.75
[Aromatics + alkanes]	19.82	19.52	1.54
Gases + H_2O + coke	16.86	15.87	6.24

20 wt.%, which is 31% more than the moisture remaining in the biomass after drying. The increase in moisture content in the bio-oil product can be attributed to the water generated during pyrolysis reactions. About 80 wt.% of the total condensable vapours is recovered in the spray tower. The incorporation of a high pressure vapour liquid separator with the quench tower increased the total condensable vapour recovery factor by 17.39% with a collection efficiency of 84%. Only 97% of the total condensable vapour ends up in the final bio-oil product while the remaining 3% is entrained in NCG. The combustible NCG mainly consists of H_2, CH_4, C_2H_4, CO and small amounts of light volatile organic alcohols and aldehydes, which collectively account for 66 wt.% of NCG, while CO_2 make up the remaining 34 wt.%. Residual solids from the pyrolysis process mainly consist of char (100% carbon) and unreacted biomass. The hydrotreated bio-oil generates long chained aromatics, phenolics and aliphatic compounds which amounts to about 37 wt.% bio-oil and are subsequently hydrocracked into smaller hydrocarbon molecules.

3.2. Energy efficiency

In order to effectively estimate the energy efficiency, the whole process is divided into two main sub-processes: biomass pyrolysis process (drying, fast pyrolysis and electric power generation) and bio-oil hydroprocessing (hydrotreating, hydrocracking and aqueous reforming).

3.2.1. Energy efficiency of fast pyrolysis process

The total energy input (E_B) into the biomass pyrolysis process is estimated from the energy content in pine wood of 25 wt.% wet basis in terms of its calorific value [26] and mass flow rate, which is about 11.32 MW. The electricity input requirement (W_{input}) for dryer air blower, pyrolysis air blower, compressors and bio-oil pumps is 0.08 MW. The energy content (E_{BO}) of fast pyrolysis bio-oil in terms of its $\text{HHV}_{\text{bio-oil}}$ [9] and mass flow rate is estimated to be 7.56 MW. Furthermore, the amount of 0.24 MW of electric power is generated from the steam cycle (W_{HE}).

The efficiency of fast pyrolysis without electricity generation, η'_p, is determined as

$$\frac{E_{\text{BO}}}{E_B + w_{\text{Input}}} = 66.3\%$$

Next, the net electrical efficiency, η'_{el}, is determined as

$$\frac{W_{\text{HE}}}{E_B + w_{\text{Input}}} = 2.1\%$$

Table 7
Stream summary of whole process.

Component (wt.%)	Dried biomass	Dryer exhaust	NCG	Bio-oil	Char	Fuel
Nitrogen	–	73.45	82.00	0.17	–	–
Oxygen	–	21.94	–	–	–	–
Hydrogen	–	–	0.33	0.00	–	–
Methane	–	–	1.73	0.00	–	–
Ethylene	–	–	1.63	0.05	–	–
Carbon monoxide	–	–	6.31	0.00	–	–
Carbon dioxide	–	–	6.21	0.19	–	–
Water	–	4.61	0.19	20.41	–	–
Levoglucosan	–	–	–	47.94	–	–
HAA	–	–	0.00	3.26	–	–
Glyoxal	–	–	0.11	0.63	–	–
Acetaldehyde	–	–	0.24	0.15	–	–
HMFU	–	–	–	1.81	–	–
Acetone	–	–	0.52	1.09	–	–
Acrylic	–	–	0.00	0.01	–	–
Xylan	–	–	–	0.35	–	–
Formaldehyde	–	–	0.62	3.46	–	–
Phenol	–	–	0.00	0.73	–	–
Methanol	–	–	0.02	2.66	–	–
Ethanol	–	–	0.16	1.24	–	–
pCoumaryl	–	–	0.00	1.47	–	–
L-Phenol	–	–	0.00	1.36	–	–
Naphthenes	–	–	–	–	–	70.00
Aromatic	–	–	–	–	–	12.00
n/i-Alkanes	–	–	–	–	–	18.00
Cellulose	–	–	–	–	24.64	–
Hemicellulose	–	–	–	–	15.01	–
Lignin Derivatives	–	–	–	12.34	1.14	–
Biomass	100	–	–	–	–	–
Char	–	–	0.00	0.65	54.03	–
Ash	–	–	0.00	0.00	5.17	–
Total mass flow (kg/h)	2489	10,800	3045	1608	337	590

Table 8
Composition of various biomasses [28].

Component	Pine wood	Switch grass	Poplar	Pine bark
Cellulose	0.42	0.36	0.47	0.22
Hemicellulose	0.23	0.31	0.22	0.23
Lignin	0.24	0.18	0.20	0.47
Water	0.10	0.10	0.10	0.06
Ash	0.01	0.05	0.01	0.02

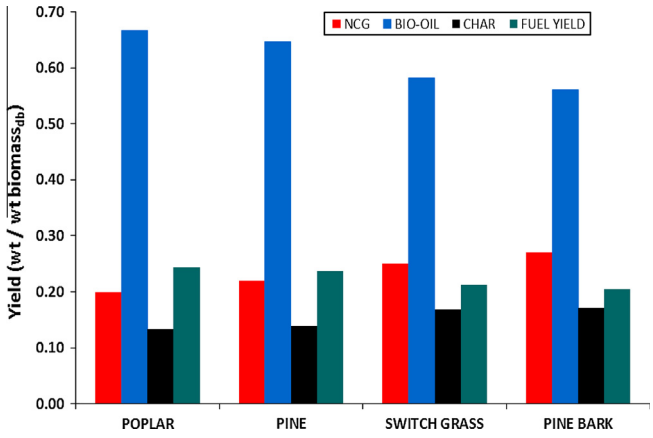

Fig. 8. Fast pyrolysis products and biofuel yield from various biomasses.

The overall energy efficiency of the fast pyrolysis process with electric power generation, $\acute{\eta}_{pel}$, is determined as $\acute{\eta}_p + \acute{\eta}_{el} = 68.4\%$.

The energy efficiency of the process without electric power generation is 66.3% which increases by 2.1% when a steam cycle is integrated with the fast pyrolysis process to generate electricity. However, the marginal increase in efficiency as a result of power generation may not be sufficient to justify the additional investment in power generation equipment.

3.2.2. Energy efficiency of bio-oil hydroprocessing

Energy content (E_{Bo}) in the pyrolysis bio-oil is 7.56 MW and energy content of supplementary natural gas ($E_{N.G}$) fed to the aqueous reformer is 0.35 MW. The total electricity input requirement (W_{input}) for hydroprocessing pumps and compressors is 0.1 MW. The energy content (E_{Fuel}) of the product biofuel is 7 MW. Thus, the local energy efficiency of the bio-oil hydroprocessing plant is 88% and the overall energy efficiency of the process of converting biomass into biofuel products and electric power is 62%.

3.3. Effect of feed composition

Various biomass feeds were compared with pine wood to examine the effect of feed types in terms of their cellulose, hemicellulose and lignin compositions on fast pyrolysis products and biofuel yields. The composition of various biomasses used in the comparative simulation is shown in Table 8. The effect of the biomass composition on fast pyrolysis products and biofuel yield is presented in Fig. 8. It was observed that poplar produces the highest bio-oil yield at 67 wt.% while pine bark produces the lowest bio-oil yield at 56 wt.%, which in turn results in significant variation in the amount of fuel produced from each biomass with the highest fuel yield (wt/wt biomass feed$_{db}$) observed for poplar at 25 wt.% and the lowest fuel yield observed for pine bark at 21 wt.%. The NCG yield follows an opposite trend with the highest yield at 27 wt.% observed for pine bark and lowest yield of 20 wt.% for poplar. Also, the highest char yield is obtained from pine bark at 17 wt.% and the lowest char yield is observed for poplar at 13 wt.%.

The amount of electricity generated from each biomass was also investigated, and is depicted in Fig. 9. It was found that the highest electricity of 0.30 MW is generated from pine bark while the lowest electricity of 0.22 MW is generated from poplar.

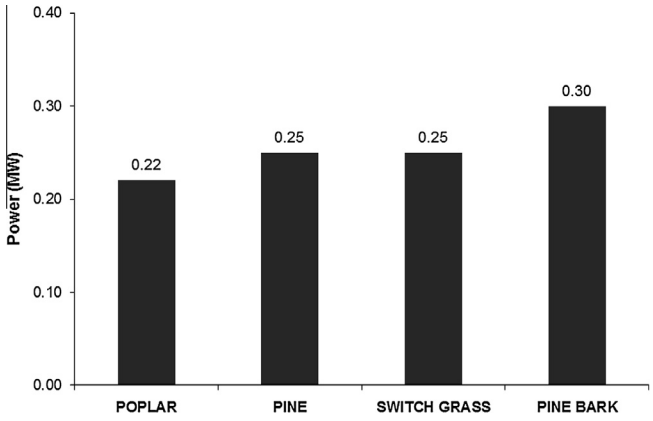

Fig. 9. Electric power generated from various biomass.

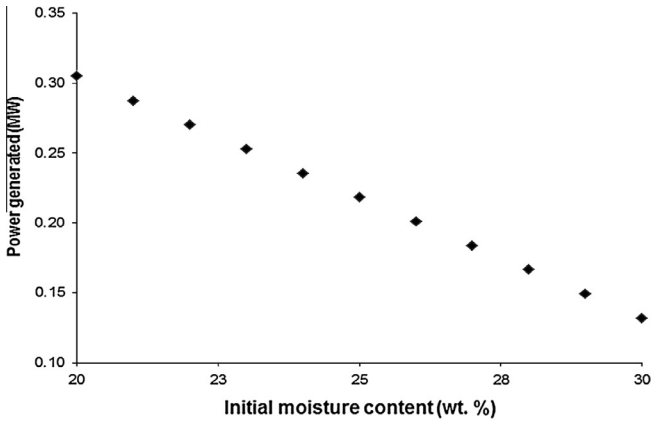

Fig. 10. Effect of initial moisture content in biomass on power generated in the process.

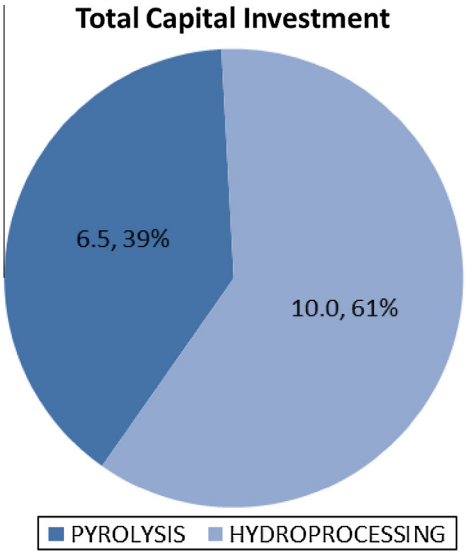

Fig. 11. Proportion of capital investment for pyrolysis and hydroprocessing.

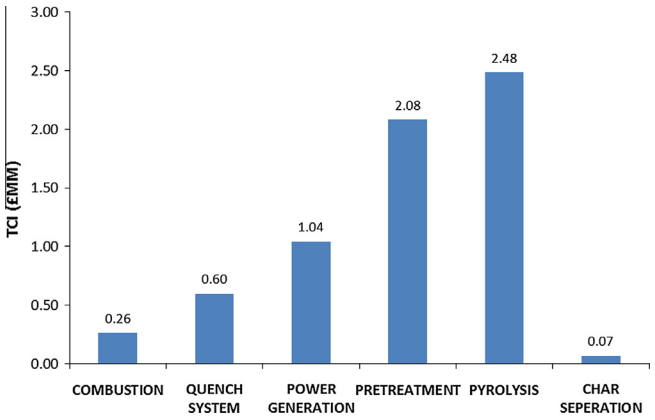

Fig. 12. Total capital investment of pyrolysis plant according to technical areas.

Table 9
Economic results.

Parameter	Value
Plant size (MT/day)	72
Total capital investment (£ MM)	16.6
Annual operating cost (£ MM)	6.4
Fuel yield (MMGGE/Year)	1.9
Product value (£/GGE)	6.25

3.4. Effect of initial biomass moisture content

The initial moisture content in biomass has no significant effect on product yields, as it is reduced to 10% prior to its entry into the pyrolysis reactor, but it has an effect on the amount of combustion waste heat available for electric power generation. The impact of initial biomass moisture content on the amount of electric power generated from the process is explored by varying moisture content between 20 and 30 wt.%. As expected, the higher the initial moisture content in the biomass, the more energy is required to reduce its moisture content to 10% as required in the pyrolysis reactor. The effect of the initial moisture content in biomass on the amount of heat available for power generation is depicted in Fig. 10, implying that the initial moisture content of the biomass has an effect on the overall efficiency of the process.

3.5. Economic analysis

3.5.1. Economic results

Total capital investment (C_{TCI}) for the 72 MT/day pine wood fast pyrolysis, bio-oil hydroprocessing and hydrogen production plant is estimated at £16.6 million, which accrues from the summation of Total Direct Cost (C_{TDC}), indirect cost (C_{TIDC}), project contingency and working capital. The percentage of contribution to C_{TCI} from the two main sub-processes, including the fast pyrolysis and bio-oil hydroprocessing, is presented in Fig. 11. The results indicate that the upgrading process accounts for 61% of C_{TCI} at £10 million, while the pyrolysis accounts for the remaining 39% at £6.6 million.

The proportion of C_{TCI} for various process units in the fast pyrolysis process is shown in Fig. 12 which reveals that the pyrolysis and pre-treatment sections account for most of the capital investment required for the fast pyrolysis process, which are about 2.48 and 2.08 £MM respectively, while char separation and combustion contribute the lowest to C_{TCi} in the fast pyrolysis sub-process i.e. 0.07 and 0.26 £MM respectively.

The result of the economic analysis is presented in Table 9. Annual operating cost for the plant is estimated at £6.4 million which accounts for operating labour cost, maintenance cost, supervision cost, utilities cost and raw material cost. In addition, catalysts replacement cost of £7.6 million is applied in the first and tenth production years assuming a 10 year catalyst lifespan. Hydrocarbon (gasoline and diesel) fuel yield for the plant is 1.9 million gallons per year and electric power generated per annum is 2.01 GW h. Income is generated from the sales of hydrocarbon fuels and the excess electricity produced. Electricity price is assumed at £0.15/kW h based on average market rates [26]. The fuel product value (PV) is obtained at zero Net Present Value (NPV) based on a 10% discount rate. Product value for this plant is observed at £6.25 per GGE when the NPV is zero.

3.5.2. Sensitivity analysis

To evaluate the effect of process and economic parameters on the economic performance of the process, a sensitivity analysis was conducted for a ±20% change in fuel yield, operating cost, electricity generated, capital investment and tax as shown in Figs. 13 and 14. Product value (PV) has the highest sensitivity to variation in fuel yield; increases of 10% and 20% in fuel yield result in 9% and 17% decrease in PV respectively. Conversely, 10% and 20% decrease in fuel yield result in 11% and 25% increase in PV respectively. Operating cost was observed to have the second highest

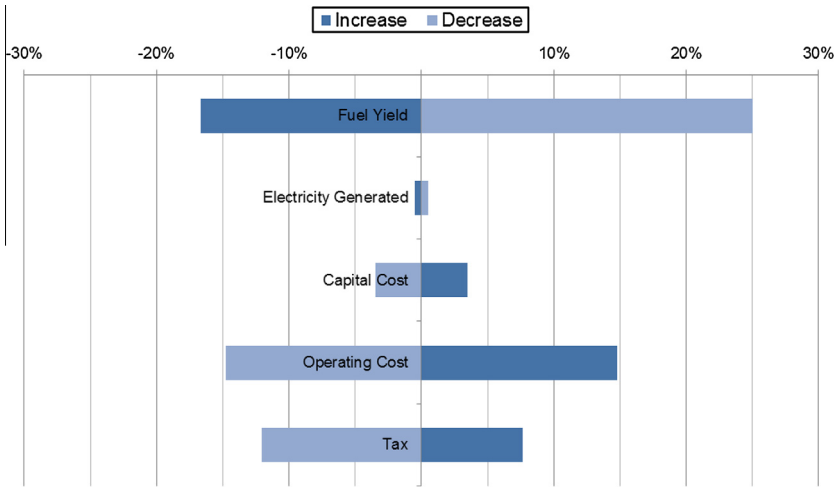

Fig. 13. Percentage difference in fuel product value over a ±20% change (increase/decrease) in process and economic parameters.

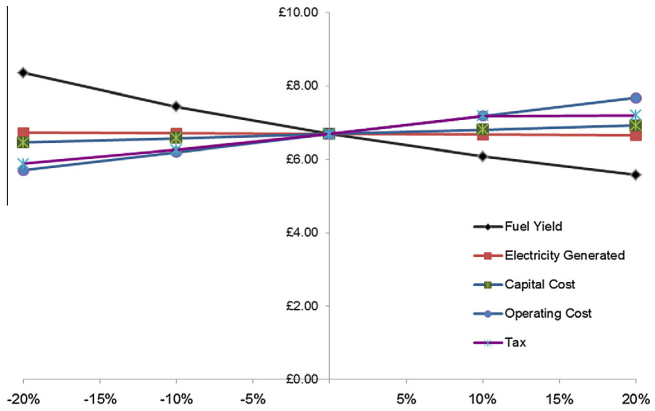

Fig. 14. Fuel product value sensitivity to process and economic parameters.

impact on PV, with increases of 10% and 20% in operating cost resulting in 7% and 15% increase in PV respectively, and *vice versa*.

PV increased by 7.34% and 7.66% when tax was increased by 10% and 20% respectively. On the other hand, PV decreased by 6.40% and 12.06% when tax was decreased by 10% and 20% respectively. Variation in capital investment indicates a relatively marginal impact on PV compared to other parameters, with 10% and 20% increase in capital investment resulting in 1.4% and 3% increase in PV respectively and *vice versa*. The lowest impact on PV was observed for electricity generated, with 10% and 20% increases in electricity generated yielding 0.48% and 0.90% decrease in PV respectively, and *vice versa*.

4. Conclusions

A high fidelity process model of a 72 MT/day pine wood fast pyrolysis and bio-oil upgrading plant was built in Aspen Plus® and validated with experimental data from literature. Major conclusions drawn from this study are as follows:

- Simulation results indicate an overall energy efficiency of 62% for an integrated plant while the local energy efficiencies of the biomass fast pyrolysis process with and without electric power generation indicates 66.3% and 68.4% respectively.
- The inclusion of power generation equipment increased the total capital investment of the pyrolysis process by 16% whilst generating only 0.24 MW which contributes a 2.1% increase to energy efficiency, hence it does not justify additional capital investment in power generation equipment; nevertheless, the amount of energy available for power generation is highly dependent of the amount of moisture in the biomass.
- The amount of moisture in the biomass has an effect of the overall energy efficiency of the process, suggesting that prior dried biomass is more suitable to increase the overall energy efficiency of the process. Also, the process heat integration can be further explored to improve the energy efficiency of the whole process.
- Economic analysis indicates that gasoline and diesel products can be produced from biomass fast pyrolysis and bio-oil hydroprocessing at a product value of £6.25/GGE and require total capital investment and annual operating costs of £16.6 million and £6.4 million respectively based on Q1. 2013 cost year over a 20 year project cycle and a 10% annual discount rate.
- The bio-oil upgrading process contributes about 61% to total capital investment while fast pyrolysis accounts for the remaining 39%; thus further equipment optimisation may be required to minimise capital cost in the hydroprocessing section.
- Sensitivity analysis of process parameters indicates that the fuel product value is mostly susceptible to changes in fuel yield, operating cost and tax while capital investment and electric power generated show a minimal impact on product value. Since catalyst development for upgrading bio-oil is being researched extensively, any new advances in low cost catalysts to improve fuel yield will reduce the cost of production significantly. Furthermore, tax breaks from government will have a significant impact on the process commercial viability, and ultimately its outlook.

Acknowledgements

The authors gratefully acknowledge the financial support for this work by the UK Engineering and Physical Sciences Research Council (EPSRC) project grant: EP/K036548/1 and FP7 Marie Curie iComFluid project grant: 312261.

References

[1] British Petroleum. BP energy outlook 2030; 2014. <http://www.bp.com/content/dam/bp/pdf/Energy-economics/Energy-Outlook/BP_Energy_Outlook_Booklet_2013.pdf> [accessed 08/25].
[2] Demirbaş A. Biomass resource facilities and biomass conversion processing for fuels and chemicals. Energy Convers Manage 2001;42(11):1357–78.
[3] IEA. From 1st to 2nd generation biofuels technologies: an overview of current industry and RD & D activities. Paris, France: International Energy Agency; 2008.
[4] Naik SN, Goud VV, Rout PK, Dalai AK. Production of first and second generation biofuels: a comprehensive review. Renew Sustain Energy Rev 2010;14(2):578–97.
[5] Food and agriculture organization of the UN. FAO food price index; 2013. <http://www.fao.org/worldfoodsituation/foodpricesindex/en/> [accessed 03/27].
[6] Furimsky E. Hydroprocessing challenges in biofuels production. Catal Today 2013;217:13–56.
[7] Bridgwater AV. Principles and practice of biomass fast pyrolysis processes for liquids. J Anal Appl Pyrol 1999;51(1–2):3–22.
[8] Bridgwater AV, Meier D, Radlein D. An overview of fast pyrolysis of biomass. Org Geochem 1999;30(12):1479–93.
[9] Bridgwater AV. Review of fast pyrolysis of biomass and product upgrading. Biomass Bioenergy 2012;38:68–94.
[10] Furimsky E. Catalytic hydrodeoxygenation. Appl Catal A 2000;199(2):147–90.
[11] Carlson T, Vispute T, Huber G. Green gasoline by catalytic fast pyrolysis of solid biomass derived compounds. ChemSusChem 2008;1(5):397–400.
[12] Wang X, Kresten SRA, Prins W, Van Swaaij PMW. Biomass pyrolysis in a fluidized bed reactor. Part 1: Literature review and model simulations. Ind Eng Chem Res 2005(23):8773–85.
[13] Gregoire CE, Bain RL. Technoeconomic analysis of the production of biocrude from wood. Biomass Bioenergy 1994;7(1–6):275–83.
[14] Cottam M, Bridgwater AV. Techno-economic modelling of biomass flash pyrolysis and upgrading systems. Biomass Bioenergy 1994;7(1–6):267–73.
[15] Islam MN, Ani FN. Techno-economics of rice husk pyrolysis, conversion with catalytic treatment to produce liquid fuel. Bioresour Technol 2000;73(1):67–75.
[16] Mullaney H, Farag H, LaClaire C, Barrett C. Technical, environmental and economic feasibility of bio-oil in New Hampshire's North Country. 14B316 UDKEIF, NHIRC, Durham; 2002.
[17] Jones SB, Holladay JE, Valkenburg C, Stevens DJ, Walton CW, Kinchin C, Elliott DC, Czernik ES. Production of gasoline and diesel from biomass via fast pyrolysis, hydrotreating and hydrocracking: a design case, PNNL-18284, PNNL, Oakridge; February 2009.
[18] Wright MM, Daugaard DE, Satrio JA, Brown RC. Techno-economic analysis of biomass fast pyrolysis to transportation fuels. Fuel 2010;89(Supplement 1): S2–S10. no. 0.
[19] Ranzi E, Faravelli T, Frassoldati A, Migliavacca G, Pierucci S, Sommariva S. Chemical kinetics of biomass pyrolysis. Energy Fuels 2008(6):4292.
[20] Wang X, Kresten SRA, Prins W, Van Swaaij PMW. Biomass pyrolysis in a fluidized bed reactor. Part 2: Experimental validation of model results. Ind Eng Chem Res 2005(23):8786–95.
[21] Sheu YE, Anthony RG, Soltes EJ. Kinetic studies of upgrading pine pyrolytic oil by hydrotreatment. Fuel Process Technol 1988;19(1):31–50.
[22] Li H, Chen Q, Zhang X, Finney KN, Sharifi VN, Swithenbank J. Evaluation of a biomass drying process using waste heat from process industries: a case study. Appl Therm Eng 2012;35:71–80.
[23] Fournol AB, Bergougnou MA, Baker CGJ. Solids entrainment in a large gas fluidized bed. Can J Chem Eng 1973;51(4):401–4.
[24] Marker TL. Opportunities for biorenewables in oil refineries. Final Technical Report. United States. DOEGO15085, UOP, Des Plaines, IL; 2005.

[25] Elliott DC, Hart TR, Neuenschwander GG, Rotness LJ, Zacher AH. Catalytic hydroprocessing of biomass fast pyrolysis bio-oil to produce hydrocarbon products. Environ Prog Sustainable Energy 2009;28(3):441–9.
[26] Biomass Energy Centre. Fuel cost per kW h; 2014. <http://www.biomassenergycentre.org.uk/portal/page?_pageid=75,59188&_dad=portal> [accessed 08/20].
[27] Sigma-Aldrich. Platinum on alumina; 2014. <http://www.sigmaaldrich.com/catalog/product/aldrich/205974?lang=en&region=GB> [accessed 08/25].
[28] ECN Phyllis2. Database for biomass and waste; 2014. <https://www.ecn.nl/phyllis2/Browse/Standard/ECN-Phyllis> [accessed 08/25].